Large Amplitude Free Vibration of Simply Supported Antisymmetric Cross-Ply Plates

Gajbir Singh* and G. Venkateswara Rao*
Vikram Sarabhai Space Centre, Trivandrum 695022, India
and
N. G. R. Iyengar†
Indian Institute of Technology, Kanpur 208016, India

The presence of bending-extension coupling in antisymmetric cross-ply plates results in the cubic nonlinear term in addition to the fourth-power term in the energy balance equation. The existence of this term does not allow two real, equal, and opposite roots while solving the energy balance equation for maximum amplitude position unlike in isotropic, orthotropic, symmetric cross-ply and symmetric and antisymmetric angle-ply plates. A direct numerical integration method has been proposed to study the large amplitude free vibrations of such plates. It is also shown that the extensively used perturbation method fails, depending on the severity of the bending-extension coupling term. Large amplitude free vibration characteristics are obtained in this paper for several configurations of antisymmetric cross-ply plates.

Nomenclature

$A_{11},A_{12},A_{22},A_{66}$	=	extensional stiffness coefficients
a, b	=	length and width of plate
B_{11}	=	bending-extension coupling stiffness coefficient
$D_{11},D_{12},D_{22},D_{66}$	=	bending stiffness coefficients
E_L,E_T	=	tensile moduli of lamina in filament and transverse directions
G_{LT}	=	shear modulus of lamina
M_1,M_2,M_6	=	moments resultants
m,n	=	half-sine waves in x and y directions
N_1,N_2,N_6	=	stress resultants
T	=	kinetic energy
T_{NL}	=	nonlinear time period
T_o	=	linear time period
t	=	time
t_i	=	thickness of ith layer
U	=	strain energy
$u,v,w,$	=	midplane displacements in x, y, and z directions
u_o,v_o,w_o	=	maximum displacements at any instant of time
W_{max}	=	maximum excitation amplitude
$\bar{W}_{max}$	=	maximum amplitude opposite to the excitation direction
x,y,z	=	Cartesion coordinates
α	=	linear stiffness coefficient
β	=	quadratic nonlinearity coefficient
γ	=	cubic nonlinearity coefficient
$\epsilon_1,\epsilon_2,\epsilon_6$	=	midplane strains
$\kappa_1,\kappa_2,\kappa_6$	=	midplane curvatures
ρ_i	=	density of ith layer
ω	=	nonlinear radian frequency
ω_o	=	linear radian frequency

Superscript

$(\dot{})$	=	differentiation with respect to time

Received Aug. 22, 1989; revision received Jan. 26, 1990.

*Scientist/Engineer, Structural Design and Analysis Division, Structural Engineering Group.
†Professor, Department of Aeronautical Engineering.

Introduction

THE advent of new stiff, strong, and lightweight composite materials, consisting of high-performance fibers unified by advanced binders, has played a key role in the success of the aerospace and aircraft industry. However, the analysis of composite structures is a complex task when compared to the conventional metallic structures because composite structures are anisotropic and are characterized by bending-extension coupling. These structures are very often subjected to severe large amplitude free vibration behavior. The topic has attracted many researchers, and a number of approximate analytical and numerical methods have been developed to study the behavior of antisymmetric cross-ply plates that commonly occur in practical structures such as solar panels, antennas, and fins, etc.

A comprehensive survey of large amplitude free vibrations of beams and plates using approximate analytical and numerical methods (finite element) has been presented by Sathyamoorthy.[1-3] A wealth of information on nonlinear response of structures is available in a standard book by Chia.[4] Large amplitude free vibration behavior of orthotropic plates was studied by Ambartsumyan[5] and Hassert and Nowinski.[6] Wu and Vinson[7,8] evaluated the nonlinear frequencies of orthotropic and symmetric laminates using Berger's[9] approach. Whitney and Leissa[10] recognized the effects of bending-extension coupling in nonlinear dynamic plate theory. Bennett[11] presented the large amplitude free vibration behavior of angle-ply plates. The large amplitude response of cross-ply and angle-ply laminates using[9] two-term perturbation method was studied by Chandra and Raju.[12-14] Sun and Chin[15] investigated the static and dynamic behavior of unsymmetric cross-ply laminates in cylindrical bending. Nonlinear vibrations of unsymmetrically laminated beams were studied by Kapania and Raciti,[16] wherein the dynamic finite element equations are reduced to a scalar equation, and a perturbation method was used to compute the frequency ratios. Sun and Chin[15] and Kapania and Raciti[16] demonstrated that a soft-spring type of nonlinearity is possible for unsymmetric laminates for certain boundary conditions. Reddy and Chao[17] presented the finite element solution for the large amplitude vibrations of anisotropic composite plates.

The energy equation for an antisymmetric cross-ply laminate contains cubic- and fourth-power nonlinear terms leading to two real but unequal (magnitude) roots unlike isotropic, orthotropic, symmetric cross-ply and symmetric/antisymmet-

ric angle-ply laminates, where the absence of cubic nonlinear terms gives two real, equal, and opposite roots. The perturbation method used by Chandra and Raju[12-14] may fail depending on the magnitude of the coefficient of their cubic nonlinear term, in other words, when bending-exetension coupling is more pronounced. In this paper, a direct numerical integration method is proposed to study the large amplitude free vibration behavior of such plates, where the bending-extension coupling is predominant. The method does not exhibit the previously mentioned problem and leads to very accurate results. The effects of this additional cubic term in the energy balance equation, which could cause a softening and hardening type of behavior are brought out. Further, the effects of aspect ratio, modulus ratio, number of layers, and lay-up sequence are also presented.

Formulation and Solution

Consider a thin rectangular plate of total thickness t composed of orthotropic layers, directed along the x and y axis, alternatively. The origin of the Cartesian coordinate system is located in the midplane with z axis being perpendicular to this plane, as shown in Fig. 1. The material of each layer is assumed to possess a plane of elastic symmetry parallel to midplane (x-y plane). The nonlinear strain-displacement relations (von Kármán type) are

$$\begin{Bmatrix} \epsilon_1 \\ \epsilon_2 \\ \epsilon_6 \end{Bmatrix} = \begin{Bmatrix} \dfrac{\partial u}{\partial x} + \dfrac{1}{2}\left(\dfrac{\partial w}{\partial x}\right)^2 \\ \dfrac{\partial v}{\partial y} + \dfrac{1}{2}\left(\dfrac{\partial w}{\partial y}\right)^2 \\ \dfrac{\partial u}{\partial y} + \dfrac{\partial v}{\partial x} + \dfrac{\partial w}{\partial x}\dfrac{\partial w}{\partial y} \end{Bmatrix} \tag{1a}$$

$$\begin{Bmatrix} \kappa_1 \\ \kappa_2 \\ \kappa_6 \end{Bmatrix} = - \begin{Bmatrix} \dfrac{\partial^2 w}{\partial x^2} \\ \dfrac{\partial^2 w}{\partial y^2} \\ \dfrac{2\partial^2 w}{\partial x \partial y} \end{Bmatrix} \tag{1b}$$

The stress and moment resultants per unit length for an antisymmetric cross-ply laminate ($B_{22} = -B_{11}$) are given by

$$\begin{Bmatrix} N_1 \\ N_2 \\ N_6 \\ M_1 \\ M_2 \\ M_6 \end{Bmatrix} = \begin{bmatrix} A_{11} & A_{12} & 0 & B_{11} & 0 & 0 \\ A_{12} & A_{22} & 0 & 0 & -B_{11} & 0 \\ 0 & 0 & A_{66} & 0 & 0 & 0 \\ B_{11} & 0 & 0 & D_{11} & D_{12} & 0 \\ 0 & -B_{11} & 0 & D_{12} & D_{22} & 0 \\ 0 & 0 & 0 & 0 & 0 & D_{66} \end{bmatrix} \begin{Bmatrix} \epsilon_1 \\ \epsilon_2 \\ \epsilon_6 \\ \kappa_1 \\ \kappa_2 \\ \kappa_6 \end{Bmatrix} \tag{2}$$

The strain energy and kinetic energy of such a plate can be written as

$$U = \tfrac{1}{2}\int_0^a\int_0^b \{A_{11}\epsilon_1^2 + 2A_{12}\epsilon_1\epsilon_2 + A_{22}\epsilon_2^2 + A_{66}\epsilon_6^2 + 2B_{11}\epsilon_1\kappa_1 - 2B_{11}\epsilon_2\kappa_2 + D_{11}\kappa_1^2 + 2D_{12}\kappa_1\kappa_2 + D_{22}\kappa_2^2 + D_{66}\kappa_6^2\}\, dx\, dy \tag{3}$$

$$T = \tfrac{1}{2}\int_0^a\int_0^b (\Sigma\rho_i t_i)\dot{w}^2\, dx\, dy \tag{4}$$

(neglecting in-plane inertia).

The following admissible functions satisfy the kinematic constraints of a simply supported plate with immovable edges:

$$u = u_o(t)\sin\frac{2m\pi}{a} \times \sin\frac{n\pi}{b}y \tag{5a}$$

$$v = v_o(t)\sin\frac{m\pi}{a} \times \sin\frac{2n\pi}{b}y \tag{5b}$$

$$w = w_o(t)\sin\frac{m\pi}{a} \times \sin\frac{n\pi}{b}y \tag{5c}$$

Substituting Eqs. (1) and (5) into Eqs. (3) and (4) and integrating gives the total strain energy U and kinetic energy, T. Applying Hamilton's principle, i.e., taking variation of $T-U$, leads to two algebraic and one second-order ordinary differential equations in terms of u_o, v_o, and w_o. Substituting u_o and v_o in terms of w_o, obtained from the first two equations, into the third equation results in a second-order nonlinear ordinary differential equation with quadratic and cubic nonlinear terms as follows

$$(\Sigma\rho_i t_i)\ddot{w}_o + \alpha w_o + \beta w_o^2 + \gamma w_o^3 = 0 \tag{6}$$

with

$$\alpha = T_8 + \frac{2T_1T_2T_5 - T_3T_5^2 - T_1^2T_6}{T_3T_6 - T_2^2}$$

$$\beta = T_9 + 3\frac{T_2T_4T_5 + T_1T_2T_7 - T_3T_5T_7 - T_1T_4T_6}{T_3T_6 - T_2^2}$$

$$\gamma = T_{10} + \frac{4T_2T_4T_7 - 2T_3T_7^2 - 2T_4^2T_6}{T_3T_6 - T_2^2}$$

where T_1, $T_2 \ldots T_{10}$ are defined in the Appendix.

Multiplying Eq. (6) by $\dot{w}_o$ and integrating with respect to time, the following energy balance equation is obtained.

$$(\Sigma\rho_i t_i)\dot{w}_o^2 + \alpha w_o^2 + \tfrac{2}{3}\beta w_o^3 + \tfrac{1}{2}\gamma w_o^4 = H = \text{const} \tag{7}$$

Linear Free Vibrations

For the case of small amplitude vibrations (linear analysis), the coefficients β and γ are set to zero. Hence, the constant H for the linear vibration case at $w_o = W_{\max}$ ($\dot{w}_o = 0$) can be obtained easily as

$$H = \alpha W_{\max}^2 \tag{8}$$

Substituting Eq. (8) into Eq. (7) with $\beta = \gamma = 0$, leads to two real and opposite roots. Hence, the linear time period or frequency can be computed as follows

$$\dot{w}_o = \frac{dw_o}{dt} = \sqrt{\alpha(W_{\max}^2 - w_o^2)/\Sigma\rho_i t_i}$$

or

$$dt = \frac{dw_o}{\sqrt{\alpha(W_{\max}^2 - w_o^2)/\Sigma\rho_i t i}} \tag{9}$$

Integrating the right side of Eq. (9) from zero to maximum amplitude gives one quarter of the time period, hence,

$$T_o = \frac{2\pi}{\omega_o} = 4\int_0^{W_{\max}} \frac{dw_o}{\sqrt{\alpha(W_{\max}^2 - w_o^2)/\Sigma\rho_i t_i}} \tag{10}$$

Substituting $w_o = W_{\max}\sin\theta$ and changing the integration limits suitably from 0 to $\pi/2$, Eq. (10) results in

$$T_o = \frac{2\pi}{\omega_o} = \frac{2\pi}{\sqrt{\alpha/\Sigma\rho_i t_i}} \tag{11}$$

Large Amplitude Free Vibrations

When the plate is undergoing large dynamic deflections, the coefficients β and γ can not be neglected as in the linear free vibration case. The constant H in this case at $w_o = W_{\max}$ becomes

$$H = \alpha W_{\max}^2 + \tfrac{2}{3}\beta W_{\max}^3 + \tfrac{1}{2}\gamma W_{\max}^4 \tag{12}$$

Substituting this constant H from Eq. (12) into Eq. (7) leads to

$$(\Sigma\rho_i t_i)\dot{w}_o^2 = \alpha(W_{\max}^2 - w_o^2) + \tfrac{2}{3}\beta(W_{\max}^3 - w_o^3) + \tfrac{1}{2}\gamma(W_{\max}^4 - w_o^4) \tag{13}$$

In the absence of coefficient β Eq. (13) at $\dot{w}_o = 0$ has two real, equal, and opposite roots. Of course, one among them is $W_{\max}$ itself; hence, the other real root is $-W_{\max}$. By following the same procedure of linear vibrations, one can evaluate the nonlinear period or frequency as

$$T_{\mathrm{NL}} = \frac{2\pi}{\omega} = 4\int_0^{\pi/2} \frac{d\theta}{\sqrt{(\alpha/\Sigma\rho_i t_i)[1 + (\gamma/2\alpha)(1 + \sin^2\theta)W_{\max}^2]}} \tag{14}$$

In the presence of coefficient β, Eq. (13) at $\dot{w}_o = 0$ will result in two real roots, one among them will be $W_{\max}$ itself, but the other one will be $-\bar{W}_{\max}$ ($W_{\max} \neq \bar{W}_{\max}$). The magnitude of $\bar{W}_{\max}$ depends on the sign and magnitude of β. Hence, the large amplitude free vibration characteristic of such plates is that the amplitude of the half cycle involving positive deflections, here onward termed as amplitude in the positive z direction, is different from the amplitude of the half cycles involving negative deflections, here onward termed as amplitude in the negative z direction of the plate. Further, this coefficient is the deciding factor for the softening or hardening type of nonlinearity, whereas in the absence of β, the nonlinearity is always of the hardening type.

To evaluate the nonlinear period/frequencies of such plates, the other real root is computed using the Newton-Raphson method, then half the period is computed with integration limits $0 \rightarrow W_{\max}$ and the other half with $0 \rightarrow -\bar{W}_{\max}$ as follows

$$T_{\mathrm{NL}} = \frac{2\pi}{\omega} = 2\left\{\int_0^{W_{\max}} \frac{dw_o}{\sqrt{(\alpha/\Sigma\rho_i t_i)[(W_{\max}^2 - w_o^2) + \tfrac{2}{3}(\beta/\alpha)(W_{\max}^3 - w_o^3) + \tfrac{1}{2}(\gamma/\alpha)(W_{\max}^4 - w_o^4)]}} + \int_0^{-\bar{W}_{\max}} \frac{dw_o}{\sqrt{(\alpha/\Sigma\rho_i t_i)[(\bar{W}_{\max}^2 - w_o^2) - \tfrac{2}{3}(\beta/\alpha)(\bar{W}_{\max}^3 + w_o^3) + \tfrac{1}{2}(\gamma/\alpha)(\bar{W}_{\max}^4 - w_o^4)]}}\right\} \tag{15}$$

Substituting $w_o = W_{\max}\sin\theta$ in the first integral and $w_o = -\bar{W}_{\max}\sin\theta$ in the second integral leads to

$$T_{\mathrm{NL}} = 2\left\{\int_0^{\pi/2} \frac{d\theta}{\sqrt{\alpha/\Sigma\rho_i t_i[1 + \tfrac{2}{3}(\beta/\alpha)(1 + \sin\theta + \sin^2\theta)/(1 + \sin\theta)W_{\max} + \tfrac{1}{2}(\gamma/\alpha)(1 + \sin^2\theta)W_{\max}^2]}} + \int_0^{\pi/2} \frac{d\theta}{\sqrt{\alpha/\Sigma\rho_i t_i[1 - \tfrac{2}{3}(\beta/\alpha)(1 + \sin\theta + \sin^2\theta)/(1 + \sin\theta)\bar{W}_{\max} + \tfrac{1}{2}(\gamma/\alpha)(1 + \sin^2\theta)\bar{W}_{\max}^2]}}\right\} \tag{16}$$

The integrands in the present paper are computed using a five-point Gaussian quadrature. It may be observed that no solution is assumed in time while deriving this expression for nonlinear period/frequency.

Chandra[13] solved Eq. (6) using a perturbation technique for small finite amplitudes to yield the following solution:

$$\left(\frac{\omega}{\omega_o}\right)^2 = 1 + \left[\frac{3}{4}\frac{\gamma}{\alpha} - \frac{5}{6}\frac{\beta^2}{\alpha^2}\right]W_{\max}^2 \tag{17}$$

The solution suggests that the sign of the amplitude does not affect the nonlinear frequency, whereas from the energy equation, it is very clear that energy is amplitude direction dependent. Further, this method fails when β is large, that is,

$$\left[\frac{3}{4}\frac{\gamma}{\alpha} - \frac{5}{6}\frac{\beta^2}{\alpha^2}\right]W_{\max}^2 \leq -1 \tag{18}$$

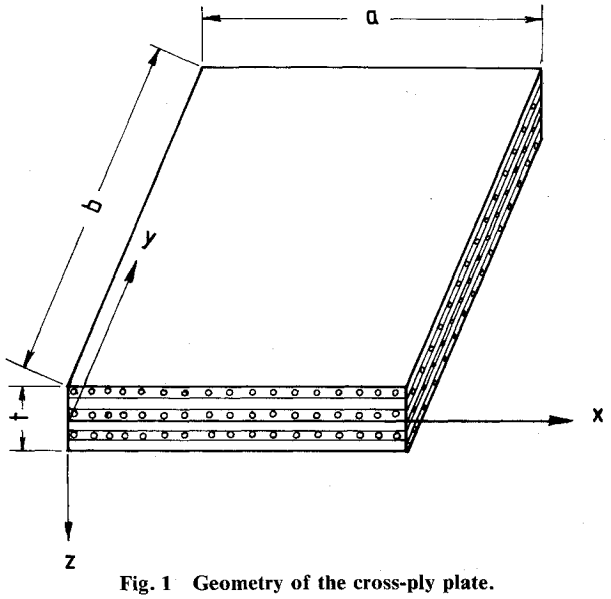

Fig. 1 Geometry of the cross-ply plate.

Results and Discussion

Based on Eqs. (11) and (16), numerical results for the variation of nonlinear to linear frequencies are presented for antisymmetric cross-ply plates having different lay ups, modular ratios, and aspect ratios for various amplitudes. Results for isotropic and symmetric cross-ply plates (for which $\beta = 0$) are also given to bring out the effectiveness of the present formulation and the cubic nonlinear term.

Tables 1 and 2 give the variation of nonlinear to linear frequency ratios with amplitude for isotropic and two-layered cross-ply plates. It can be seen that frequency ratios (ω/ω_o) obtained from the proposed method compare well with those obtained using the perturbation method[18] for isotropic plates ($a/b = 1$ and 2) and for the square two-layered cross-ply plate (0 deg/90 deg). It may be observed that the perturbation method fails for the two-layered cross-ply rectangular plates beyond a certain amplitude. This is because of the assumption that the plate vibrates with the same amplitude at $t = 0, 2\pi/\omega, 4\pi/\omega\ldots$, is same as at $t = \pi/\omega, 3\pi/\omega\ldots..$), which is not true, as has been shown in the text: Eq. (13) does not have equal and opposite real roots.

The nonlinear frequency ratios at various amplitude ratios for a square two-layered cross-ply plate are compared with the

Table 1 Comparison of nonlinear to linear frequency ratios for isotropic plates ($\nu = 0.3$)

W_{max}/t	ω/ω_o					
	Square plate			Rectangular plate $a/b = 2.0$		
	Numerical integration	Perturbation method	Ref. 18	Numerical integration	Peturbation method	Ref. 18
0.2	1.0208	1.0208	1.0196	1.0254	1.0254	1.0241
0.4	1.0805	1.0809	—	1.0975	1.0981	—
0.6	1.1724	1.1743	1.1642	1.2072	1.2097	1.1998
0.8	1.2893	1.2937	—	1.3447	1.3505	—
1.0	1.4248	1.4327	1.4097	1.5022	1.5124	1.4903
2.0	2.2508	2.2828	—	2.4425	2.4798	—

Table 2 Comparison of nonlinear to linear frequency ratio for two-layered cross-ply plates ($E_L/E_T = 40$; $G_{LT}/E_T = 0.5$; $\nu_{LT} = 0.25$)

W_{max}/t	ω/ω_o			
	Square plate		Rectangular plate $a/b = 2.0$	
	Numeical integration	Perturbation method[13]	Numerical integration	Perturbation method[13]
0.3	1.0796	1.0801	0.9448	0.8896
0.6	1.2867	1.2910	0.9568	0.4069
0.9	1.5691	1.5811	1.1432	[a]
1.2	1.8933	1.9148	1.4376	
1.5	2.2414	2.2731	1.7826	
1.8	2.6040	2.6458	2.1521	
2.1	2.9759	3.0277	2.5341	
2.4	3.3541	3.4157	2.9235	
2.7	3.7366	3.8079	3.3172	
3.0	4.1223	4.2032	3.7137	

[a] Perturbation method fails.

Table 3 Comparison of nonlinear to linear frequency ratio for square two-layered cross-ply plate ($E_L = 7.07 \times 10^6$; $E_T = 3.58 \times 10^6$; $G_{LT} = 1.41 \times 10^6$; $\nu_{LT} = 0.3$)

W_{max}/t	ω/ω_o		
	Numerical integration	Perturbation method	Finite element[17]
0.6	1.1904	1.1926	1.18[a]
1.2	1.6263	1.6399	1.62[a]
1.8	2.1619	2.1912	2.15[a]
2.4	2.7399	2.7854	2.75[a]

[a] values deduced from graph.

finite element results of Reddy and Chao[17] in Table 3. The results obtained from the proposed direct numerical integration method, perturbation method, and finite element method agree well with each other.

A phase-plane diagram (w_o vs $\dot{w}_o$) for isotropic and two-layered cross-ply plates with aspect ratios 1 and 2 is shown in Fig. 2. It can be seen that in the case of an isotropic plate this plot is a symmetric ellipse and its area reduces with increase in aspect ratio. For the two-layered cross-ply square plate, again, the phase-plane diagram is a symmetric ellipse, but for a similar rectangular plate of aspect ratio 2, this diagram is not symmetric about the $\dot{w}_o$ axis. It may be observed that if the initial excitation amplitude is 1.0, the plate oscillates with + 1.0 amplitude in the initial excitation direction and − 0.58 in the opposite direction. The amplitude in the direction opposite to the initial excitation will increase if the lay up is interchanged, that is, (0 deg/90 deg) becomes (90 deg/0 deg). Similar conclusions can be drawn from Fig. 3, which shows the variation of amplitude with respect to time for two-layered cross-ply plates having aspect ratios 1 and 2. It can be seen that the period for the positive deflection half cycle is large when compared to the negative deflection half cycle for a rectangular two-layered cross-ply plate, whereas for a square plate, it is the same. In fact, the nonlinear to linear period ratios can be calculated from this figure also.

The effects of number of layers and lay-up sequence and initial excitation direction for a rectangular cross-ply plate of aspect ratio 2 is shown in Fig. 4. Four-layered symmetric cross-ply $(0 \text{ deg}/90 \text{ deg})_s$ and $(90 \text{ deg}/0 \text{ deg})_s$ plates reveal that they are independent of amplitude direction and form upper and lower bounds, respectively, compared to the antisymmetric lay ups having more than four layers. The effect of the

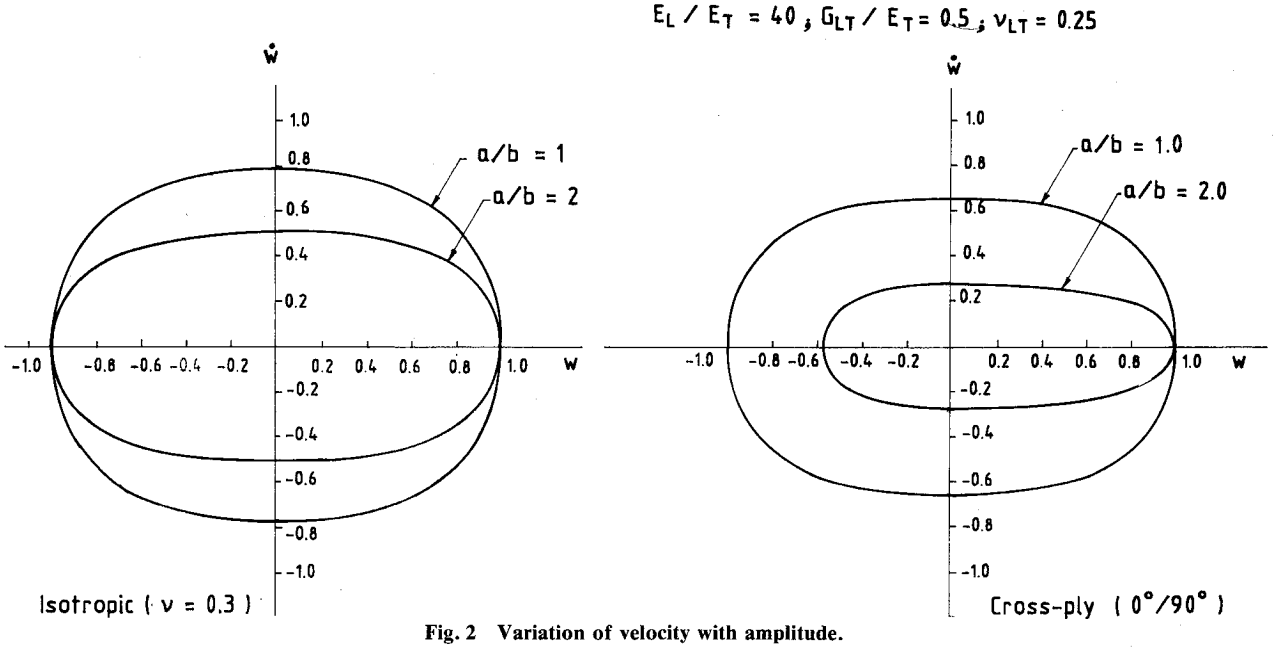

Fig. 2 Variation of velocity with amplitude.

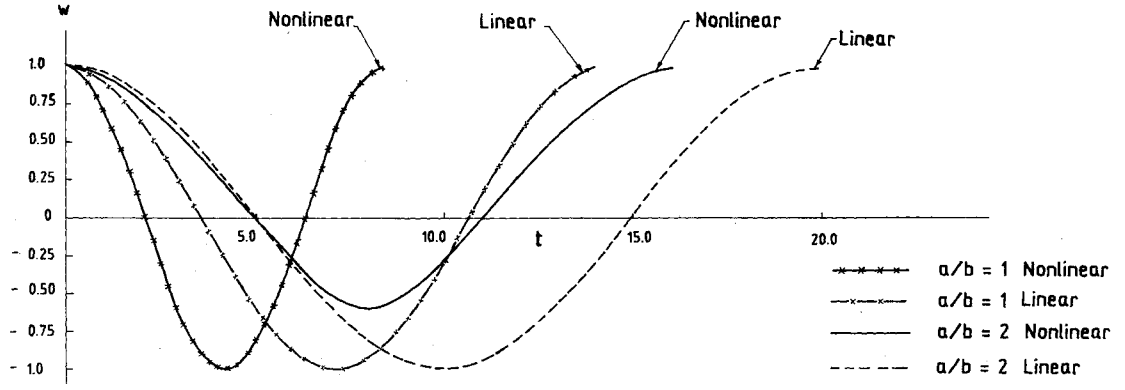

Fig. 3 Variation of amplitude with time.

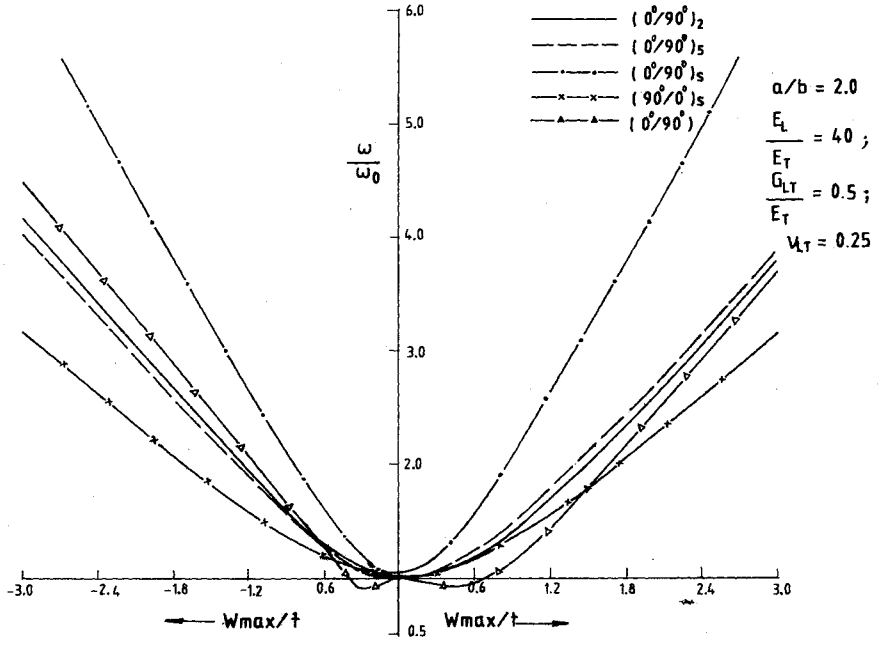

Fig. 4 Nonlinear to linear frequency ratio vs amplitude ratio for various lay ups.

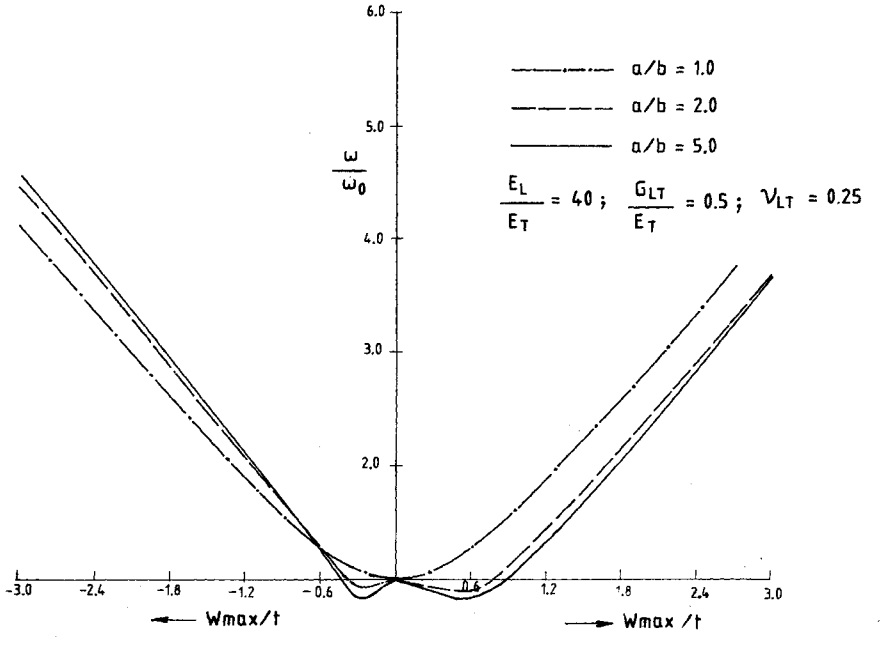

Fig. 5 Nonlinear to linear frequency ratio for various aspect ratios.

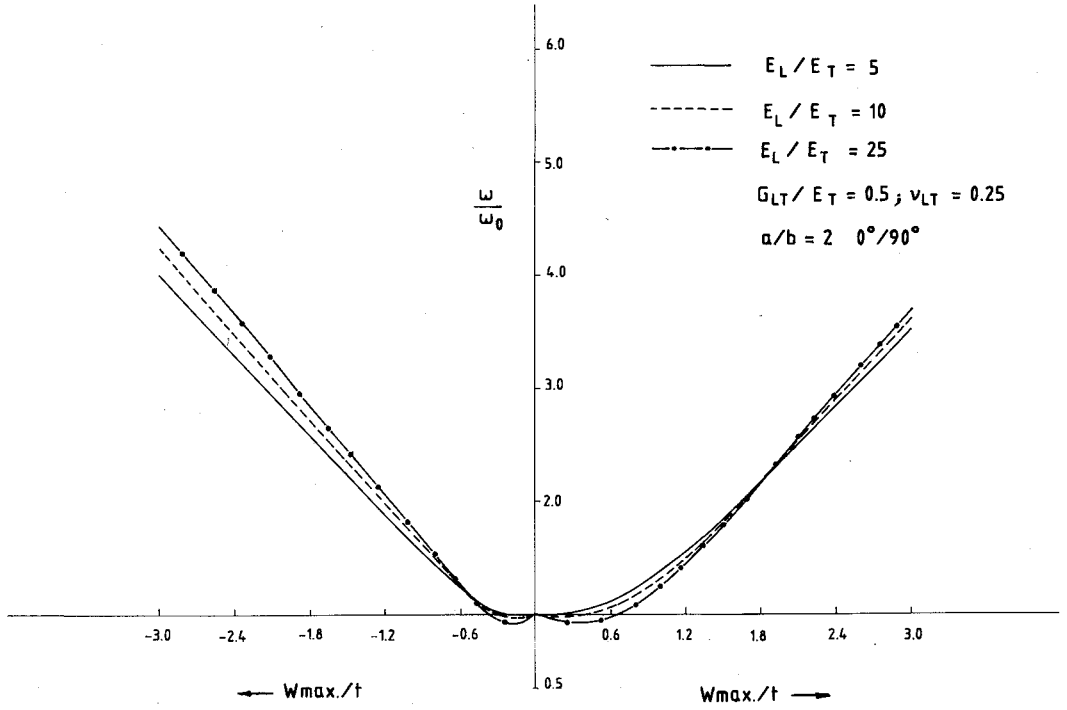

Fig. 6 Nonlinear to linear frequency ratio vs amplitude ratio for various modular ratios.

cubic nonlinear term in Eq. (7) is to reduce the hardening type of nonlinearity for positive initial excitation amplitudes and vice versa. For this reason, two-layered cross-ply rectangular plates show softening for small initial excitation amplitudes and then hardening. Further, the nonlinearity increases with the increase in number of layers for positive initial excitation amplitudes and reduces with negative ones; the reverse is true for antisymmetric plates having (90 deg/0 deg...) sequence.

Figure 5 shows the effect of aspect ratio and amplitude direction for a two-layered (0 deg/90 deg) cross-ply plate. It may be observed that a square two-layered plate does not show any softening type of nonlinearity and is independent of amplitude direction because of the fact that the cubic nonlinear term in energy Eq. (7) vanishes for this case. The plates with high aspect ratio show that there is softening for the initial excitation amplitudes and then hardening. Further, the nonlinearity reduces with increase in aspect ratio for positive excitation amplitudes and increases for negative excitation amplitudes.

The effects of modular ratio on nonlinear frequencies for two-layered rectangular ($a/b = 2.0$) cross-ply plates are presented in Fig. 6. It can be seen that the softening nonlinearity amplitude region increases with increase in modular ratio since the bending-extension coupling increases and, hence, increases the severity of the cubic nonlinear term in the energy Eq. (7). Further the asymmetry about ω/ω_o axis increases with increase of modular ratio.

Conclusions

The proposed direct numerical integration method results in very accurate predictions of nonlinear frequencies for rectangular antisymmetric cross-ply composite plates. The perturbation method used by many investigators fails to yield any meaningful results when bending-extension coupling is large. The rectangular ($a/b > 1.0$) antisymmetric cross-ply plates show softening type of nonlinearity for initial small amplitudes and then hardening type of nonlinearity under immovable edge conditions, and the amplitude of vibration at $t = 0$, $2\pi/\omega$, $4\pi/\omega$, ...etc. is different from the one at $t = \pi/\omega$, $3\pi/\omega$,...etc. The initial softening type of nonlinearity is the result of bending-extension coupling and boundary conditions. The range of amplitudes for which the softening nonlinearity results for antisymmetric cross-ply plates increases with the increase in aspect ratio and modular ratio and decreases with increase in number of layers. The time period for the positive deflection half cycle is large for a rectangular antisymmetric cross-ply plate, whereas for a square plate it is the same for positive deflection half cycle and negative deflection half cycle.

Appendix: Expressions for T_i ($i = 1, 2,...10$)

$$T_1 = \frac{4C_n}{3n\pi}\left(\frac{n\pi}{b}\right)^3 B_{11}$$

$$T_2 = \frac{16C_{mn}}{9mn\,\pi^2}\left(\frac{m\pi}{a}\right)\left(\frac{n\pi}{b}\right)(A_{12}+A_{66})$$

$$T_3 = 4\left(\frac{n\pi}{b}\right)^2 A_{22} + \left(\frac{m\pi}{a}\right)^2 A_{66}$$

$$T_4 = \frac{C_m}{3m\pi}\left[2\left(\frac{n\pi}{b}\right)^3 A_{22} - \left(\frac{m\pi}{a}\right)^2\left(\frac{n\pi}{b}\right)(A_{12}-A_{66})\right]$$

$$T_5 = \frac{-4C_m}{3m\pi}\left(\frac{m\pi}{a}\right)^3 B_{11}$$

$$T_6 = 4\left(\frac{m\pi}{a}\right)^2 A_{11} + \left(\frac{n\pi}{b}\right)^2 A_{66}$$

$$T_7 = \frac{C_n}{3n\pi}\left[2\left(\frac{m\pi}{a}\right)^3 A_{11} - \left(\frac{m\pi}{a}\right)\left(\frac{n\pi}{b}\right)^2(A_{12}-A_{66})\right]$$

$$T_8 = \left(\frac{m\pi}{a}\right)^4 D_{11} + 2\left(\frac{m\pi}{a}\right)^2\left(\frac{n\pi}{b}\right)^2\left(D_{12}+2D_{66}\right) + \left(\frac{n\pi}{b}\right)^4 D_{22}$$

$$T_9 = \frac{4C_{mn}}{3mn\,\pi^2}\left[\left(\frac{m\pi}{a}\right)^4 B_{11} - \left(\frac{n\pi}{b}\right)^4 B_{11}\right]$$

$$T_{10} = \frac{9}{32}\left[\left(\frac{m\pi}{a}\right)^4 A_{11} + \frac{1}{16}\left(\frac{m\pi}{a}\right)^2\left(\frac{n\pi}{b}\right)^2(A_{12}+2A_{66}) + \left(\frac{n\pi}{b}\right)^4 A_{22}\right]$$

where

$$C_n = 1-(-1)^n$$

$$C_m = 1-(-1)^m$$

$$C_{mn} = C_m C_n$$

References

[1]Sathyamoorthy, M., "Nonlinear Analysis of Beams, Part-I: A Survey of Recent Advances," *Shock and Vibration Digest,* Vol. 14, No. 7, 1982, pp. 19-35.

[2]Sathyamoorthy, M., "Nonlinear Analysis of Beams, Part-II: Finite Element Methods," *Shock and Vibration Digest*, Vol. 14, No. 8, 1982, pp. 7-18.

[3]Sathamoorthy, M., "Nonlinear Vibrations of Plates—A Review," *Shock and Vibration Digest*, Vol. 15, 1983, No. 6, pp. 3-16.

[4]Chia, C. Y., *Nonlinear Analysis of Plates*, McGraw-Hill, New York, 1980.

[5]Ambartsumyan, S. A., *Theory of Anisotropic Plates* (English translation), Technomic, Stanford, CT, 1970.

[6]Hassert, J. E., and Nowinski, J. L., "Nonlinear Transverse Vibration of a Flat Rectangular Orthotropic Plate Supported by Stiff Ribs," *Proceedings of the 5th International Symposium on Space Technology and Science*, Tokyo, 1962, pp. 561-570.

[7]Wu, C. I., and Vinson, J. R., "On Nonlinear Oscillations of Plates Composed of Composite Materials," *Journal of Composite Materials,* Vol. 3, No. 6, 1969, pp. 548-561.

[8]Wu, C. I., and Vinson, J. R., "Nonlinear Oscillations of Laminated Specially Orthotropic Plates with Clamped and Simply Supported Edges," *Journal of the Acoustical Society of America*, Vol. 49, No. 5(2), 1971, pp. 1561-1567.

[9]Berger, H. M., "A New Approach to the Analysis of Large Deflection of Plates," *Journal of Applied Mechanics,* Vol. 22, 1955, pp. 465-472.

[10]Whitney, J. M., and Liessa, A. W., "Analysis of Heterogeneous Anisotroic Plates," *Journal of Applied Mechanics,* Vol. 36, No. 2, 1969, pp. 261-266.

[11]Bennett, J. A., "Nonlinear Vibrations of Simply Supported Angle-Ply Laminated Plates," *AIAA Journal*, Vol. 9, No. 10, 1971, pp. 1997-2003.

[12]Chandra, R., and Raju, B. B., "Large Amplitude Flexural Vibrations of Cross-Ply Laminated Comosite Plates," *Fibre Science and Technology*, Vol. 8, No. 4, 1975, pp. 243-264.

[13]Chandra, R., "Large Deflection Vibration of Cross-Ply Laminated Plates with Certain Edge Conditions," *Journal of Sound and Vibration*, Vol. 47, No. 4, 1976, pp. 509-514.

[14]Chandra, R., and Raju, B. B., "Large Deflection Vibration of Angle-Ply Laminated Plates," *Sound and Vibration*, Vol. 40, No. 3, 1973, pp. 393-408.

[15]Sun, C. T., and Chin, N., "On Large Deflection Effects in Unsymmetric Cross-Ply Composite Laminates," *Journal of Composite Materials*, Vol. 22, No. 11, 1988, pp. 1045-1059.

[16]Kapania, R. K., and Raciti, S., "Nonlinear Vibrations of Unsymmetrically Laminated Beams," *AIAA Journal,* Vol. 27, No. 2, 1989, pp. 201-210.

[17]Reddy, J. N., and Chao, W. C., "Nonlinear Oscillations of Laminated Anisotropic Rectangular Plates," *Journal of Applied Mechanics,* Vol. 49, No. 2, 1982, pp. 396-402.

[18]Dumir, P. C., and Bhaskara, A., "Some Erroneous Finite Element Formulations of Nonlinear Vibrations of Beams and Plates," *Journal of Sound and Vibration*, Vol. 123, No. 3, 1988, pp. 514-527.